CATHODIC VACUUM ARC MULTILAYER COATINGS (TiZrSiY)N/NbN: STRUCTURE AND PROPERTIES DEPENDING ON THE DEPOSITION INTERVAL OF ALTERNATE LAYERS

Vyacheslav M. Beresnev[a], Serhii V. Lytovchenko[a]*, Mykola O. Azarenkov[a,b], Olga V. Maksakova[a,c], Denis V. Horokh[a], Bohdan O. Mazilin[a], Diana Kaynts[d], Irina V. Doshchechkina[e], Oleg V. Gluhov[f]
[a] V.N. Karazin Kharkiv National University, 4, Svoboby Sq., 61022 Kharkiv, Ukraine
[b] National Science Center «Kharkov Institute of Physics and Technology», 1, Akademicheskaya St., 61108 Kharkiv, Ukraine
[c] Institute of Materials Science, Slovak University of Technology in Bratislava, 25, Jána Bottu Str., 917 24 Trnava, Slovakia
[d] Uzhhorod National University, 3, Narodna Sq., 88000 Uzhhorod, Ukraine
[e] Kharkiv National Automobile and Highway University, 25, Ya. Mudryi St., 61200 Kharkiv, Ukraine
[f] Kharkiv National University of Radio Electronics, Nauki Ave. 14, 61166, Kharkiv, Ukraine
*Corresponding Author e-mail: s.lytovchenko@karazin.ua
Received October 9, revised November 20, accepted November 23, 2023

Two series of multilayer coatings with different numbers of bilayers (268 and 536, respectively) were synthesised using the cathodic vacuum-arc deposition (CVAD) with the simultaneous sputtering of two different cathodes. The first cathode was made of the multicomponent TiZrSiY material, and the second one was made of technical niobium. The coatings were condensed in a nitrogen atmosphere at a constant negative bias potential applied to the substrate. The resulting coatings have a distinct periodic structure composed of individual layers of (TiZrSiY)N and NbN with the thicknesses determined by the deposition interval (10 or 20 s, respectively). The total thicknesses of the coatings determined by the number of bilayers were 11 and 9 microns, respectively. The formation of polycrystalline TiN and NbN phases with grain size comparable to the size of the layers has been identified for both series of coatings. The layers exhibit a columnar structure growth with a predominant orientation (111). The hardness of the experimental coatings depends on the thickness of the layers and reaches 39.7 GPa for the coating with the smallest layer thickness. The friction coefficient of the obtained coatings varies from 0.512 to 0.498 and also depends on the thickness of the layers. A relatively large value of the friction coefficient is due to high roughness and the presence of a droplet fraction on the surface as well as in the volume of the coatings.

Keywords: *Cathodic vacuum-arc deposition; Multilayer coatings; Layer number; Texture; Microhardness; Tribological properties; Friction parameters*
PACS: 61.46.-w; 62.20.Qp; 62-25.-g; 81.15.Cd

INTRODUCTION

Modern high-tech production requires new materials with unique properties. In many cases, to provide the required surface properties, functional coatings formed using modern technologies are used. The application of such coatings can significantly increase equipment reliability, reduce maintenance costs, extend service life, restore working surfaces and parts, and protect against high loads and aggressive environments.

Multilayer functional coatings are one of the most effective types of protective coatings. Its characteristic feature is the difference in the physical, mechanical, and chemical properties of the constituent layers. Ion plasma deposition technologies have significant advantages in terms of creating multilayer coating systems for tribological applications.

The architecture and construction of multilayer coatings, taking into account their functions and structure, constituent materials of individual layers, their sequence, and thickness, makes it possible to control the properties of the surface (for example, hardness and elastic modulus), and therefore its functionality. Several scientific works have proposed a mechanism for increasing the hardness of multilayer coatings, based on the transition of the alternating layer thicknesses to the nanometre scale, in which the formation of dislocations is suppressed, and the difference in the elastic moduli of neighbouring layers prevent the dislocations motion [1-3].

Binary nitrides, such as TiN and ZrN coatings, have been widely used to improve the surface properties of substrate materials. They are highly resistant to hardness, wear, and corrosion, making them useful for many industrial applications. TiZrN coatings not only have a relatively higher resistance to corrosion, high adhesion, and low COF, but also excellent hardness and wear resistance. One of the ways to further improve the coating system based on the TiZrN system is to increase the number of alloying elements. Si, Y, V, Cr, and other elements can be used for this purpose. Thus, the addition of Si leads to the formation of a nanocrystalline structure and strengthening of the coating. This is consistent with the Hall-Petch relation, from which it follows that reducing the grain size to a certain critical value leads to an increase in the hardness and strength of the nitride compound [4]. At silicon concentrations of 6-8 at.%, the TiZrN coating has a nanocomposite structure characterised by the formation of an amorphous tissue Si_3N_4 [5-8]. Coatings with

high concentrations of Si are characterized by the formation of SiO_2 layers in the near-surface region, which serve as an additional barrier to the diffusion of oxygen atoms [9].

The addition of yttrium to the coating composition helps to increase oxidation due to the possible formation of the YO_2 phase at grain boundaries, as well as eliminate the formation of columnar crystals [10,11]. The simultaneous addition of Si and Y to the coating can further improve its oxidation stability, corrosion resistance, and also reduce the level of internal stresses [12].

Further improvement in the properties of multicomponent coatings based on monophase nitride systems containing Ti, Zr, Cr, Si, Y, Al or other elements can be achieved under certain formation conditions under which the increase in the hardness increases but the Young modulus decreases. Young's modulus is an important characteristic of a material, largely determining its hardness. While increased hardness is desirable for high-performance coatings for tribological applications, Young's modulus of such coatings must be low enough to improve strain resistance and thermal stability.

The formulated conditions can be met when creating a multilayer coating, where one layer is a multicomponent nitride system, for example (TiZrSiY), and the second layer is a mononitride, for example, NbN. The plastic properties of the suggested mononitride are ensured by a decrease in Young's modulus and, in some cases, an increase in heat resistance during the formation of a surface oxide film NbO_x [13].

This article reports on the application of cathodic vacuum-arc deposition [14] for the synthesis of multilayer nitride coatings based on niobium and a multi-element system (TiZrSiY) with nanoscale layers, as well as a study of the influence of the structural phase state of obtained coatings on their physical and mechanical properties.

EXPERIMENTAL DETAILS

Experimental coatings were grown by cathodic arc in a non-commercial deposition system (see Figure 1). The elemental composition of the first target was (in at. %): 72.5 Ti + 20 Zr + 5.0 Si + 2.5 Y. The second target was made of niobium with a purity of 98.2 at. Coating deposition was carried out in a nitrogen environment at a nitrogen pressure (P_N) of 0.53 Pa and a negative bias applied to the substrate (U_b) of 200 V. The substrates were made of AISI 321 steel with dimensions of $15 \times 15 \times 2,0$ mm^3).

Two series of samples with coatings based on a two-layer system (TiZrSiY)N/NbN were produced. The total thickness of the coating of the first series was about 11 μm, and that of the second series was about 9 μm. The sample of the first series contained 536 layers, and the second series contained 268 layers.
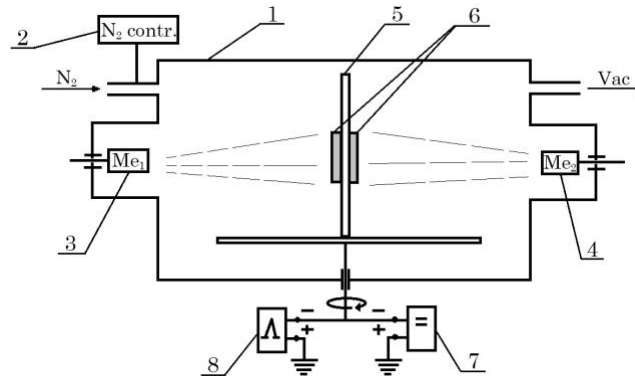

Figure 1. Scheme of the deposition unit used for the synthesis of multilayer coatings: 1 – vacuum chamber; 2 – automatic nitrogen pressure control system; 3 – TiZrSiY multielement target evaporator (Me₁); 4 – Nb target evaporator (Me₂); 5 – substrate holder; 6 - substrates; 7, 8 – DC and pulse voltage sources.

The cross-sectional microstructure of the coatings at different magnifications, as well as morphology of the surface after wear tests were studied using scanning electron microscopy in a Quanta 600 FEG and FEI Nova NanoSEM 450 microscopes. The phase state of the coatings was characterised using X-ray diffraction in a DRON-3M diffractometer in Cu-Kα radiation. Identification of the phases and calculation of main crystal structural parameters was done using Malvern Panalytical's XRD software.

The microhardness of the coatings was measured using an automated ultramicrohardness tester, called «Shiumadzu», using the Vickers indentor. The applied load was 245 mN and the holding time was 10 s. The accuracy of the measurement result according to the device's passport indicators is ± 1,5 %.

Tribological tests of the coatings were carried out in air using the 'ball-disk' scheme. The "Tribometer" device from CSM Instruments was used as a friction machine. For tribological tests, coatings were deposited on the surface of polished cylindrical samples (42 mm in diameter, 5 mm in height) made of 45 steel (surface roughness $R_a = 0,088$ microns). A ball with a diameter of 6.0 mm made of sintered certified aluminium oxide Al_2O_3 was used as a counterbody. The applied load was 6,0 H, the sliding speed was 10 sm/s. The tests comply with international standards ASTM G99-959, DIN50324 and ISO 20808.

Cathodic Vacuum ARC Multilayer Coatings (TiZrSiY)N/NbN: Structure and Properties...   **EEJP. 4 (2023)**

RESULTS AND DISCUSSION

Figure 2 shows cross-sectional SEM images of multilayer coatings (TiZrSiY)N/NbN at two magnifications. Both coatings show distinct alternating of (TiZrSiY)N and NbN layers with thicknesses of (35 ÷ 39) and (17 ÷ 22) nm (seria 1) and (36 ÷ 45) and (31 ÷ 39) nm, respectively. It should be noted that the thickness of the (TiZrSiY)N layers exceeds the thickness of the NbN layers. An explanation for this fact may be, on the one hand, a higher rate of evaporation of metals from a multielement cathode. On the other hand, the smaller thickness of NbN can also be associated with the lower formation energy of the NbN compound (213 kJ/mol) compared to TiN (337 kJ/mol).
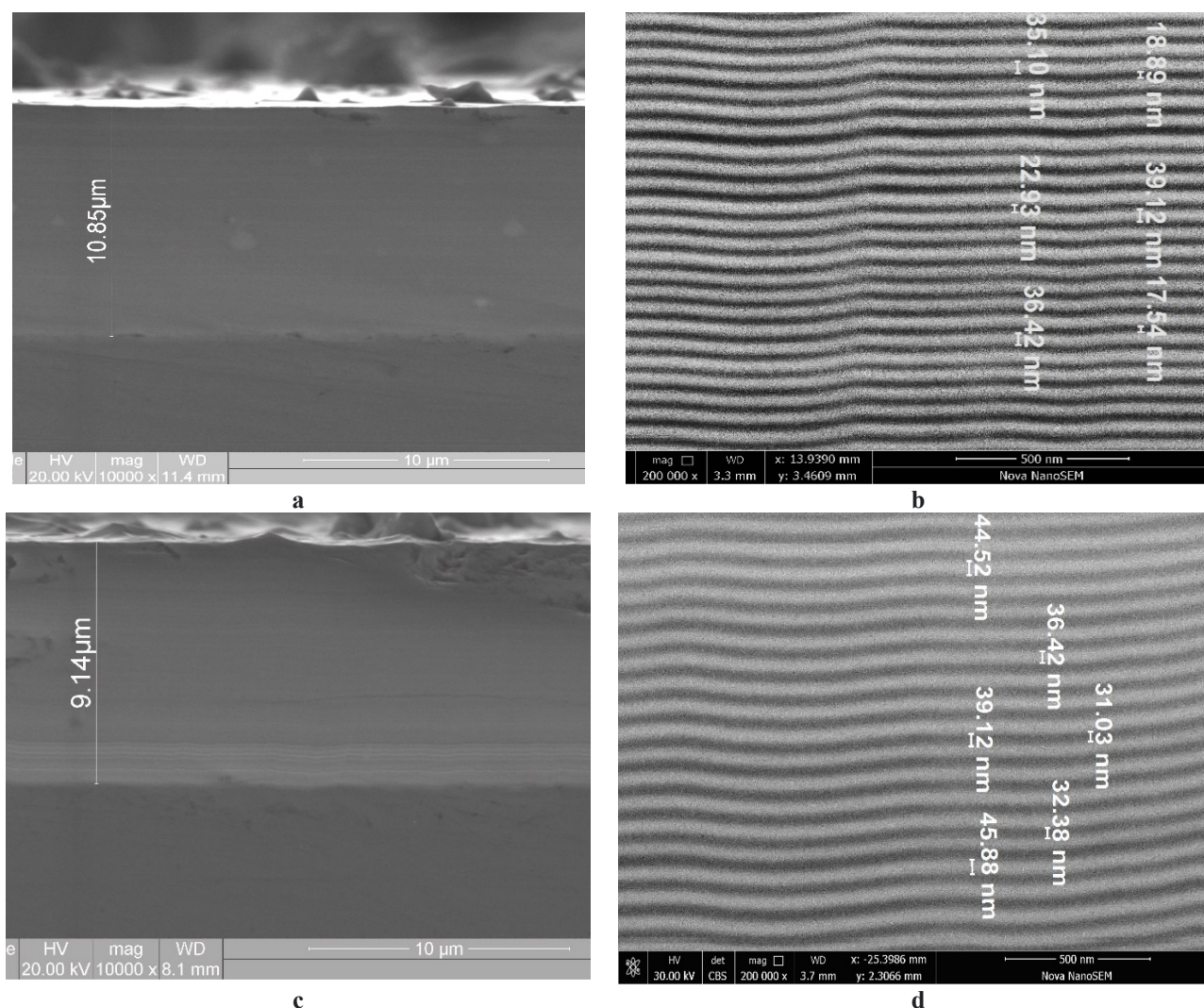

Figure 2. SEM cross section micrographs of multilayer **(TiZrSiY)N/NbN** coatings
at low (left) and high magnifications (right): seria 1 (a, b) and seria 2 (c, d)

There is some unevenness in the thickness of the layers in depth. The alternation of layers of different thicknesses is apparently due to the dynamics of the technological parameters during the coating deposition process. The characteristic waviness of the forming layers is caused in part by the presence of the droplet fraction, as well as by the influence of electromagnetic fields in the deposition area. The formation of the wavy structure of the layers is also influenced by the initial morphology of the substrate surface.

To improve the adhesive bond between the substrate and the coating, before the coating, additional cleaning of the substrate surface from adsorbed substances and oxide films was carried out using a stream of accelerated ions. Speaking about oxide films, it should be emphasised that after preliminary cleaning (mechanical treatment, ultrasonic treatment, degreasing), a layer of oxides up to 2.5 nm thick may be formed on the surface, and after heating in a vacuum to the deposition temperature of the coating, the thickness of the oxide film can increase almost in half. To remove these contaminants from the surface of the substrate, it is necessary to apply a negative bias voltage of about 10^3 V. This parameter may ensure the cleaning at the atomic level. Surface cleaning with TiZrSiY and Nb ions occurred under a high vacuum under the pressure of 0.001 Pa and with a negative potential on the substrate of 1300 V, which led to heating of the substrate and its partial sputtering. As a result, a certain amount of cathode material still settles on the surface of the substrate and diffuses to a small depth, thus forming a transition layer between the coating and the substrate, the thickness of which is 29.5 nm (see Figure 3).
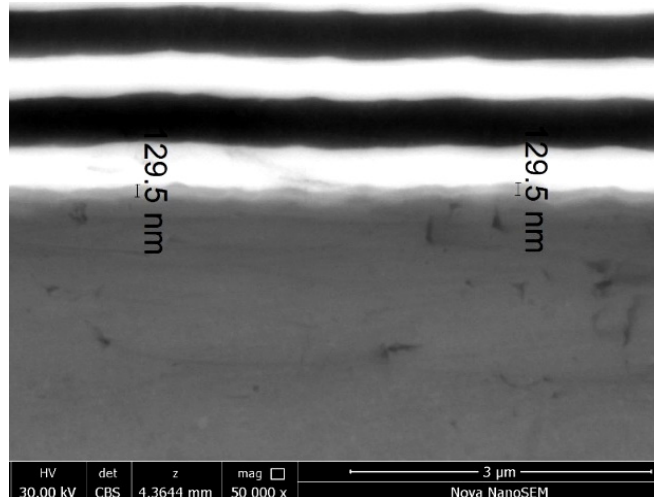
Figure 3. High-magnification SEM image of the transition zone between the substrate and multilayer **(**TiZrSiY)N/NbN coating seria 2.

The results of the X-ray diffraction analysis of multilayer (TiZrSiY)N/NbN coatings are shown in Figure 4. As one can see, the formation of complex phase structure is identified for all experimental coatings. The fcc-TiN phase with (111) and (222) planes was revealed for (TiZrSiY)N layers and mixture of hcp-NbN-ε phase (PDF-2 6-719), as well as a small amount of NbN-δ' (PDF-2 20-802) was identifies for NbN layers. The NbN-δ' phase (space group P6$_3$/mmc) having the anti-NiAs-type structure appears as a metastable structure during the phase transformation NbN-δ → NbN-ε.

In the coatings of the first seria, the lattice parameter of TiN is 0.4301 nm. The grain size of TiN is 17.9 nm and the level of microdeformation is 2.27×10^{-3}. The line intensity distribution corresponds to texture (200) with the texture coefficient Tc$_{(200)}$ = 3.97. The lattice parameters of NbN-ε are 0.2959 nm and 0.1140 nm. The grain size of NbN is 10.2 nm and the microdeformation level of microdeformation is 5.97×10^{-3}. Line intensity distribution of the line corresponds to the texture (004). The lattice parameters of NbN-δ' are 0.2988 nm and 0.5573 nm. Line intensity distribution corresponds to texture (002).
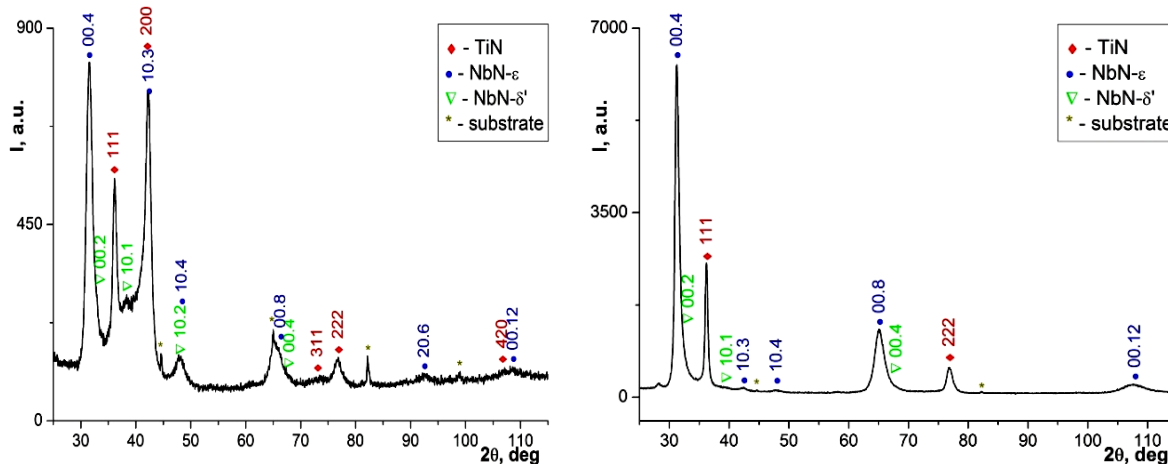

Figure 4. Diffraction patterns of multilayer **(**TiZrSiY)N/NbN coatings: seria 1 (left) and seria 2 (right)

In the coatings of the second seria, the lattice parameter of TiN is 0,4295 nm. The grain size of TiN is 20.4 nm and the level of microdeformation is 3.74×10^{-3}. The line intensity distribution corresponds to texture (111) with the texture coefficient Tc$_{(111)}$ = 6.00. The lattice parameters of NbN-ε are 0.2959 nm and 0.1145 nm. The grain size of NbN is 26.4 nm and нм the level of microdeformation is 6.70×10^{-3}. Line intensity distribution of the line corresponds to texture (004). The lattice parameters of NbN-δ' are 0.2967 nm and 0.5642 nm. Line intensity distribution corresponds to texture (002).

During the crystallisation of niobium nitride, several phases can form [17], and in most cases, NbN films have a mixed phase composition [18, 19]. Because of the complex composition and structure of the experimental coatings, the diffraction patterns contain diffraction peaks from different phases with some overlapping of the peaks.

It is known that Nb atoms dissolve in the TiN lattice to form a substitutional solid solution (TiNb)N. According to the Hume-Rothery rule, isomorphism of elements at temperatures far from the melting point appears when the difference in atomic sizes is less than 15% (the atomic radii for titanium is 0.147 nm and for niobium is 0.146 nm).

Therefore, for the experimental coatings, the predominant formation of a substitutional solid solution (TiNb)N is possible at the interfaces of (TiZrSiY)N and NbN layers. For the coatings of the first seria, obtained at a 10 s interval for the growth of each layer, the joined diffraction peak of (103)NbN-ε and (200)TiN is found at 2θ = 42.7° (see Fig. 4a). We suppose that this peak is related to the formation of a (TiNb)N solid solution (hcp crystal structure) at the interfaces of the (TiZrSiY)N and NbN layers or even the formation of interlayer transition zones between layers.

It has been revealed that the interval for the growth of each layer to 20 s (coatings of the second seria), the line intensity distribution from all peaks increases and broadening of diffraction peaks decreases (see Fig. 4b). The joined diffraction peak of (103)NbN-ε and (200)TiN as well as other diffraction peaks from NbN-ε and NbN-δ′ disappear. The line intensity of (004) NbN-ε increases dramatically. Nitride NbN-ε has a homogeneity region at nitrogen concentrations in the range of 48.0 to 50.6 at.% [17], and nitride NbN-δ′ exist at nitrogen concentrations in the range of 28.6 to 34.4 at.%. Based on these data, it can be assumed that an increase in the deposition time and, accordingly, the thickness of the layer leads to a change in the nitrogen concentration in the NbN bilayers and, as a consequence, to an increase in the volume fraction of the nitrogen-rich NbN-ε phase. In addition, the deposition time also influences the lattice parameters of the nitride phase. When the interval for the growth of each layer is 10 s (coatings of the first seria), the lattice parameter of TiN is 0.4301 nm, but when the interval for the growth of each layer is 10 s (coatings of the second seria), the lattice parameter of TiN decreases to 0.4295 nm. One can suppose that the changes in the lattice parameter point to the change in the the nitrogen content in TiZrSiYN layers. Several studies report this dependence, i.e. the decrease of the lattice parameter with a decrease in the nitrogen content. In summary, for multilayer coatings it is possible to influence the phase-structural state of the growth layers by varying the interval [20].

The change in modulation period affects the state of the interfaces of multilayer coatings, which play a decisive role in their properties [21]. Reducing the thickness of the layers while maintaining the total thickness of the coating increases the number of interfaces between layers, which act as a barrier to the migration of dislocations and the propagation of microcracks [22, 23]. The main mechanical properties of the multilayer (TiZrSiY)N/NbN coating as well as thickness ratio between the constituent layers are summarized in Table 1. The ratios H/E^* and H^3/E^{2*} are used to represent resistance against elastic strain to failure and resistance to plastic deformation, respectively.

Table 1. Mechanical properties of multilayer (TiZrSiY)N/NbN coatings

Number of seria and thickness ratio between layers, nm	Hardness H, GPa	Young modulus E^*, GPa	H/E^*	H^3/E^{2*}
seria 1: 18/36	39.7	438	0.09	0.32
seria 2: 31/45	37.1	421	0.088	0.28

The data from the table indicate that coating with a smaller layer thickness has better mechanical parameters, which is associated with the size effect and with the formation of incoherent (with different types of crystalline lattice) interphase boundary in the layers.

To study the adhesive strength of the multilayer (TiZrSiY)N/NbN coatings, we performed a sclerometric study of the best coating of the first seria using the Revetest scratch tester. The coating has been subjected to deformation (scratching) in the elastic and elastic-plastic regions to the limiting state, followed by destruction during horizontal movement of the indenter, previously embedded to a certain depth. The critical loads Lc, leading to the destructural changes during the test, have been determined as follows: (1) Lc1 corresponds to the onset of penetration of the indenter into the coating; (2) Lc2 corresponds to the appearance of the first cracks; (3) Lc3 corresponds to the appearance of clusters of cracks; (4) Lc4 characterizes the peeling of some regions of the coating, and (5) Lc5 characterizes the chipping of the coating or its plastic abrasion. According to the obtained data, the wear of the coating occurs quite evenly without the formation of avalanche chips, which can be determined by the insignificant level of acoustic emission signals with increasing load on the indenter (see Figures 5 and 6).
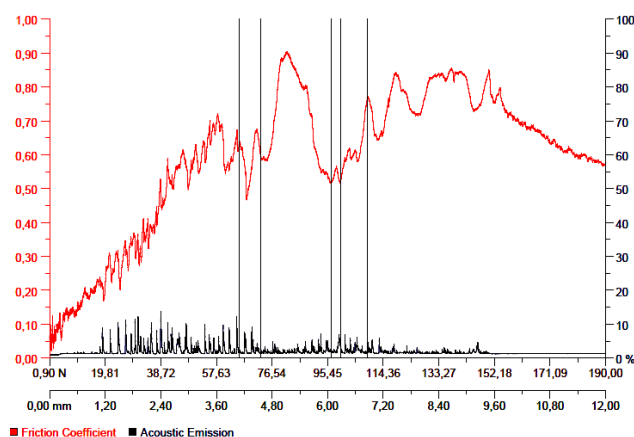

Figure 5. Results of scratch test of multilayer (TiZrSiY)N/NbN coating seria 1

The cohesive failure of the coating starts at 72.81 N, the adhesive failure is noted at 99.78 N and the full interfacial failure is registered at 109.07 N.

The results of tribological tests at room temperature during dry friction of multilayer (TiZrSiY)N/NbN coatings are given in Table 2. As can see, the friction coefficient of the coatings varies from 0.512 to 0.498. These relatively high values can be explained by the high roughness and the presence of a droplet fraction on the surface and in the volume of the coatings, the formation of which is due to the deposition technique.
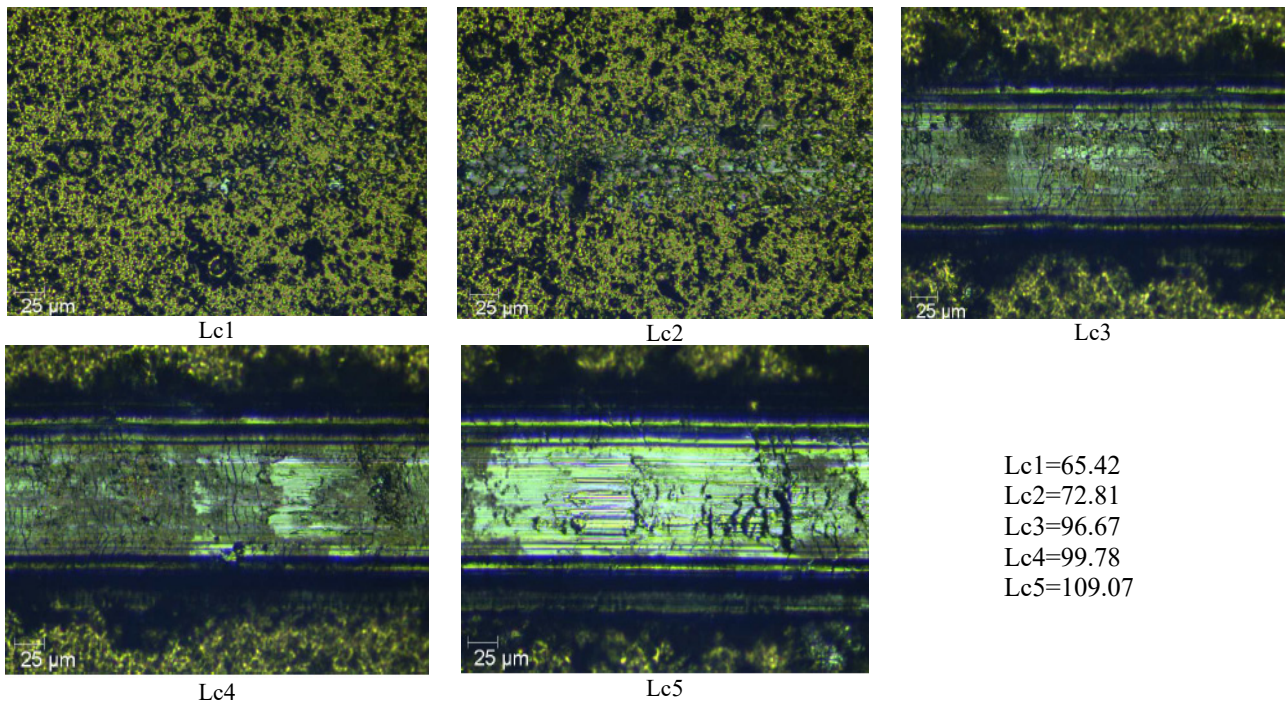

Lc1=65.42
Lc2=72.81
Lc3=96.67
Lc4=99.78
Lc5=109.07

Figure 6. Images of the scratch on the surface of multilayer (TiZrSiY)N/NbN seria 1 at different loads

Table 2. Tribological parameters of multilayer (TiZrSiY)N/NbN coatings

Number of seria and thickness ratio between layers, nm	Friction coefficient		Wear factor, mm^3×N^{-1}×m^{-1}	
	initial	tested	counterbody (×10^{-6})	coatings (×10^{-5})
seria 1: 18/36	0.318	0.498	2.2	1.4
seria 2: 31/45	0.341	0.512	2.0	1.5

When the wear tracks, some conclusions can be drawn about the wear mechanism. It is known that the main wear mechanisms of coatings are (1) adhesive wear with buildup of the coating material to the counterbody, (2) abrasive wear with the formation of grooves on the coatings surface by a more rigid counterbody, (3) tedious wear with removal of particles of the coating's material, and (4) plastic deformation of the coatings material.

The SEM image of the worn surface and the corresponding profile of multilayer (TiZrSiY)N/NbN coating seria 1 is shown in Figure 7.
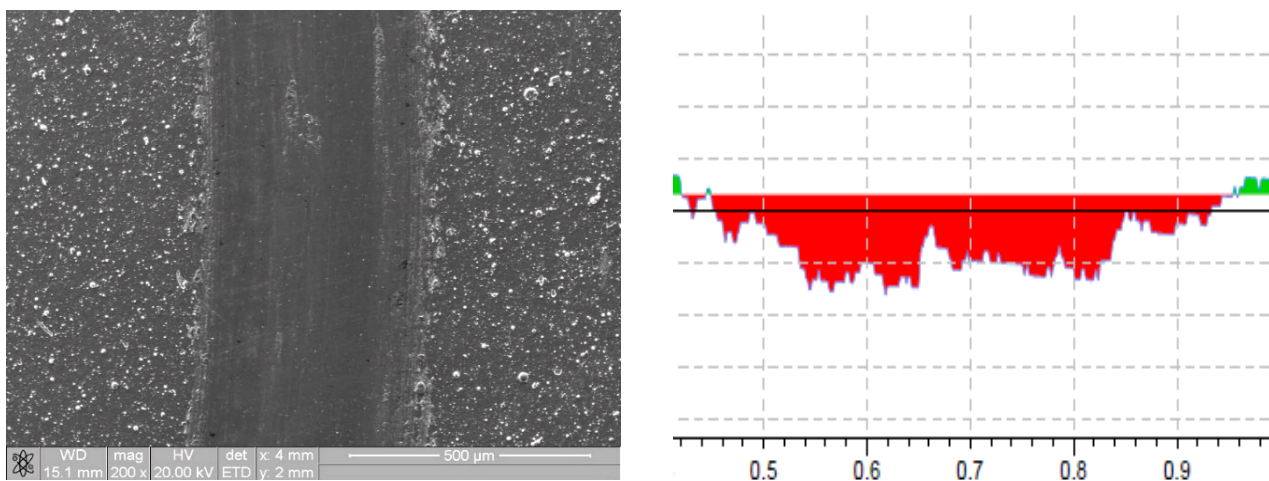

Figure 7. SEM image of the wear track and corresponding depth profile of multilayer (TiZrSiY)N/NbN coating seria 1

The nature of the wear track indicates the abrasive wear mechanism of the experimental coating. The bottom of the groove has a rather ridged structure, which is obviously associated with the presence of droplet defects in the volume of the coating.

Experimental studies indicate that under certain friction conditions, not only material transfer occurs, but also the interaction of the environment with sliding surfaces activated by friction energy. Under non-equilibrium friction conditions in air, it is possible to form a polyoxide tribofilm on the worn surface, which will contain oxidation products and the interaction of the phase components of the coating and the counterbody. It indicates that tribochemical oxidation occurred in the atmosphere.

The intensity of wear strongly depends on the hardness of the coating and the strength of the adhesive bond between the layers. It should be noted that for multilayer composite nanostructured coatings, the grain and interlayer boundaries are zones of intense energy dissipation. Cracks deviate from the direction of initial propagation and are partially or completely inhibited, which is actually a strengthening of the coating material. Furthermore, grain boundaries, which contribute to grain formation and material texture, can effectively strengthen the coating. Therefore, coatings with a nanoscale structure and multilayer architecture are characterised by longer service life, especially under conditions of cyclic thermomechanical stresses [24].

CONCLUSIONS

It is shown that in cathodic vacuum-arc multilayer (TiZrSiY)N/NbN coatings, a change in the thickness of individual layers and the bilayer period leads to a change in the lattice parameter of the nitride phases. The lattice parameter of TiN decreases with 0.4301 nm (the interval for the growth of each layer is 10 s) to 0.4295 nm (the interval for the growth of each layer is 20 s).

Experimental coatings have the complex structural state of the fcc-TiN phase and the mixture of hcp-NbN-ε and NbN-δ' phases. The increase in deposition time and, accordingly, thickness of the layers leads to a change in nitrogen concentration and, as a consequence, to an increase in the volume fraction of nitrogen-rich NbN-ε phase in NbN layers. The decrease in the deposition time results in the diffusion of NbN atoms into (TiZrSiY)N layers and the formation of a solid solution (TiNb)N phase (hcp crystal structure).

The mechanical and tribological data indicate the advantages of the coating with thinner layers (the interval for the growth of each layer is 10 s) and its high resistance to the initiation and propagation of cracks. This coating has a hardness of 39.7 GPa, Young's modulus of 438 GPa, and an adhesion strength of 99.78 N. The complete interfacial failure of the coating occurs at a critical load of 109.07 N.

Under dry conditions, both multilayer (TiZrSiY)N/NbN coatings have high wear resistance. The friction coefficients vary from 0.512 до 0.498. The wear mechanism of the experimental coating is mainly abrasive. Tribochemical oxidation in the atmosphere environment is revealed.

ORCID
Vyacheslav M. Beresnev, https://orcid.org/0000-0002-4623-3243; Serhiy V. Lytovchenko, https://orcid.org/0000-0002-3292-5468
Mykola O. Azarenkov, https://orcid.org/0000-0002-4019-4933; Olga V. Maksakova, https://orcid.org/0000-0002-0646-6704
Denis V. Horokh, https://orcid.org/0000-0002-6222-4574; Bohdan O. Mazilin, https://orcid.org/0000-0003-1576-0590
Diana Kaynts, https://orcid.org/0000-0002-7242-027X; Irina V. Doshchechkina, https://orcid.org/0000-0002-6278-7780
Oleg V. Gluhov, https://orcid.org/0000-0003-2453-5504

REFERENCES
[1] A. Cavaleiro and J.T. de Hosson, editors *Nanostructured Coatings*, (Springer-Verlag, USA, 2006). https://link.springer.com/content/pdf/bfm:978-0-387-48756-4/1?pdf=chapter%20toc
[2] A.D. Pogrebnjak, O.M. Ivasishin, and V.M. Beresnev. Uspehi Fiziki Metallov, **17**(1), 1 (2016). https://doi.org/10.15407/ufm.17.01.001
[3] M. Stueber, H. Holleck, H. Leiste, et al., J. Alloys Compd. **483**, 321 (2009) https://doi.org/10.1016/j.jallcom.2008.08.133
[4] N. Hansen. Scr. Mater. **51**, 801 (2004). https://doi.org/10.1016/j.scriptamat.2004.06.002
[5] S.Z. Li, Y. Shi, and H. Peng, Plasma Chem. and Plasma Proc. **12**, 287 (1992). https://doi.org/10.1007/BF01447027
[6] V.V. Vasil'ev, A.A. Luchaninov, E.N. Reshetnyak, V.E. Strel'nitskij, G.N. Tolmatcheva, and M.V. Reshetnyak, PAST, **2009**(2), 173 (2009). https://vant.kipt.kharkov.ua/ARTICLE/VANT_2009_2/article_2009_2_173.pdf
[7] O.D. Pohrebniak, O.V. Bondar, O.V. Sobol, and V.M. Beresnev, Soft Nanoscience Letters, **3**, 46 (2013). http://dx.doi.org/10.4236/snl.2013.33009
[8] Q. Wan, N. Liu, B. Yang, H. Liu, and Y. Chen, Journal of Wuhan University of Technology-Mater. Sci. Ed. **34,** 774 (2019). https://doi.org/10.1007/s11595-019-2116-9
[9] J. Musil, and H. Polakova. Surf. Coat. Technol. **127**, 99 (2000). https://doi.org/10.1016/S0257-8972(00)00560-0
[10] D.C. Tsai, Y.L. Huang, S.R. Lin, et al. Appl. Surf. Sci. **257,** 1361 (2010) http://dx.doi.org/10.1016/j.apsusc.2010.08.078
[11] B.D. Beake, L. Bergdoll, L. Isern, et al., Int. J. Refract. Met. Hard Mater. **95**, 105441 (2021). https://doi.org/10.1016/j.ijrmhm.2020.105441
[12] M. Li, R. Wang, Y. Fan, and L. Wang, Materials Research Innovations, **19**(8), S8–190 (2015). https://doi.org/10.1179/1432891715Z.0000000001653

[13] J. Yi, J. Xiong, Z. Guo, et al., Ceram. Int. **48**, 6208 (2022). http://dx.doi.org/10.1016/j.ceramint.2021.11.161

[14] I. Aksionov, A. Andreev, V. Belous, et al., *Вакуумная дуга: источники плазмы, осаждение покрытий, поверхностное модифицирование [Vacuum arc: plasma sources, coating deposition, surface modification]* (Naukova dumka, Kyiv, 2012). (in Russian).

[15] A. Bolgar, and V. Linvinenko, *Термодинамические свойства нитридов [Thermodynamic properties of nitrides]* (Naukova dumka, Kyiv, 1980). (in Russian).

[16] M. Azarenkov, O. Sobol`, A. Pogrebniak, and V. Beresnev, *Инженерия вакуумно-плазменных покрытий [Engineering of vacuum plasma coatings]*, (KhNU, Kharkiv, 2011). (in Russian).

[17] H. Holleck, *Binäre und ternäre Carbid- und Nitridsysteme der Übergangsmetalle. Materialkundlich-Technische Reihe*, Nr. 6 (Hrsg. G. Petzow). (Gebrüder Borntraeger, Berlin - Stuttgart, 1984).

[18] G.Y. Oya, and Y. Onodera. J. Appl. Phys. **45**, 1389 (1974). https://doi.org/10.1063/1.1663418

[19] G.Y. Oya, and Y. Onodera. J. Appl. Phys. **47**, 2833 (1976). https://doi.org/10.1063/1.323080

[20] V.M. Beresnev, S.V. Lytovchenko, D.V. Horokh, B.O. Mazilin, et. al., Journal of nano- and electronic physics. **11**(5), 05037 (2019). https://jnep.sumdu.edu.ua/download/numbers/2019/5/articles/jnep_11_5_05037.pdf

[21] M. Hock, E. Schaffer, W. Doll, and G. Kleer, Surface and Coatings Techn. **163-164**, 689 (2003). https://doi.org/10.1016/S0257-8972(02)00658-8

[22] V. Ivashchenko, S. Veprek, A. Pogrebnjak, and B. Postolnyi, Science and Technology of Advanced Materials. **15**(2), 025007 (2014). https://doi.org/10.1088/1468-6996/15/2/025007

[23] A.D. Pogrebnjak, V.I. Ivashchenko, P.L. Skrynskyy, et al., Composites Part B: Engineering, **142**, 85 (2018). https://doi.org/10.1016/j.compositesb.2018.01.004

[24] V.M. Beresnev, O.V. Sobol, S.S. Grankin, U.S. Nemchenko, et al., Inorg. Mater. Appl. Res. **7**, 388 (2016) https://doi.org/10.1134/S2075113316030047

ВАКУУМНО-ДУГОВІ БАГАТОШАРОВІ ПОКРИТТЯ (TiZrSiY)N/NbN: БУДОВА ТА ВЛАСТИВОСТІ ЗАЛЕЖНО ВІД ТРИВАЛОСТІ ОСАДЖЕННЯ ШАРІВ, ЩО ЧЕРГУЮТЬСЯ

Вячеслав М. Береснєв[a], Сергій В. Литовченко[a], Микола О. Азаренков[a,b], Ольга В. Максакова[a,c], Денис В. Горох[a], Богдан О. Мазілін[a], Діана Кайнц[d], Ірина В. Дощечкіна[e], Олег В. Глухов[f]

[a] Харківський національний університет імені В.Н. Каразіна, майдан Свободи 4, 61022, м. Харків, Україна

[b] Національний науковий центр «Харківський фізико-технічний інститут», вул. Академічна, 1, 61108, м. Харків, Україна

[c] Інститут матеріалознавства, Словацький технічний університет у Братиславі, вул. Яна Ботту, 25, 917-24, м. Трнава, Словаччина

[d] Ужгородський національний університет, вул. Народна, 3, 88000, м. Ужгород, Україна

[e] Харківський національний автомобільно-дорожній університет, вул. Ярослава Мудрого, 25, 61002, м. Харків, Україна

[f] Харківський національний університет радіоелектроніки, проспект Науки, 14, 61166, м. Харків, Україна

Вакуумно-дуговим способом при одночасному розпиленні двох катодів різного складу сформовані багатошарові покриття, що містять різну кількість подвійних шарів (бішарів, відповідно 268 і 536). Один катод був виготовлений з багатокомпонентного матеріалу TiZrSiY, а другий – з технічного ніобію. Осадження покриття проводили в азотній атмосфері за негативного потенціалу зміщення на підкладці. Отримане покриття (TiZrSiY)N/NbN має періодичну шарувату структуру з товщинами окремих шарів, що визначаються тривалістю осадження (10 або 20 с). Загальна товщина покриття визначається кількістю сформованих бішарів. Зафіксовані у покритті фази TiN і NbN є полікристалічними, розміри зерен можна порівняти з розмірами шарів. У шарах спостерігається стовпчаста структура з переважною орієнтацією (111). Твердість сформованих покриттів залежить від товщини шарів і сягає 39.7 ГПа у покритті з найменшою з отриманих товщиною шарів. На всіх зразках з покриттям залежно від товщини шарів коефіцієнт тертя змінюється від 0,512 до 0,498. Досить велика величина коефіцієнта тертя обумовлена високою шорсткістю та наявністю краплинної фракції на поверхні та в покритті.

Ключові слова: *вакуумно-дугове розпилення; багатошарові покриття; кількість шарів; текстура; мікротвердість; трибологічні властивості; фрикційні характеристики*